


Cite this: *RSC Adv.*, 2020, 10, 21406

# Recovery of niobium and tantalum by solvent extraction from Sn–Ta–Nb mining tailings†

Olga Rodríguez,<sup>a</sup> Francisco J. Alguacil,<sup>a</sup> Esther Escudero Baquero,<sup>a</sup> Irene García-Díaz,<sup>a</sup> Paloma Fernández,<sup>b</sup> Belén Sotillo<sup>b</sup> and Félix A. López<sup>\*a</sup>

The slag from the extraction processes of metals from their ores may contain valuable components that, if adequately recovered, can be reintroduced in the technological life cycle. This is the case for the material obtained in Penouta mines in the North of Spain. These mineral sites are a main source of tin obtained from cassiterite. The mineral is submitted to a pyrometallurgical process to separate tin, however cassiterite is not the only mineral present in the veins, and large amounts of other minerals are normally discarded, constituting the slag. In the present case, besides cassiterite, one of the most abundant minerals in the ore is columbo tantalite, the source of the strategic coltan. In this work the raw material (slag) has been treated by acid leaching, using HF/H<sub>2</sub>SO<sub>4</sub> as the leaching agent. Then liquid–liquid extraction of Nb and Ta was performed, with Cyanex®923 extractant, so that both metals were obtained separately. Then they were precipitated from the corresponding aqueous solution, and calcined in order to yield Nb<sub>2</sub>O<sub>5</sub> of 98.5% purity and tantalum salt, after calcination and purification, of 97.3% purity. The process described in this work opens a possibility to produce high quality materials that are considered critical by the EU from alternative sources exempt of criticality factors.

Received 14th April 2020  
Accepted 29th May 2020

DOI: 10.1039/d0ra03331f

rsc.li/rsc-advances

## Introduction

Niobium, tantalum and Rare Earth Elements (REEs) are included in the 2017 year list of the 27 critical raw materials of the European Union due to their importance for high-tech products and emerging innovations and the risk in the security of supply and economic importance (EU, 2017).<sup>1</sup> Up to 30% of the required energy to refine these metals is used just in separation processes, like liquid–liquid extraction.<sup>2,3</sup> The list of critical raw materials contains those compounds or elements that reach or exceed thresholds for both economic importance and supply risk.<sup>1</sup> Without supply security, the EU economy could be affected, because they are required in the production of the majority of technological components, and they are determinant in the competitiveness of the European industry, strongly hampered in the case of a lack of the external supply of strategic and hardly replaceable materials.

Niobium and tantalum, together with titanium, zirconium, tin, REE, thorium, uranium and alkali earth metals in different proportions, enter in the composition of about 100 different minerals.<sup>4</sup> Nowadays, the most important sources of Nb and Ta

are: tantalum niobates (salts from niobic and tantalic acids), such as columbite and tantalite, respectively.<sup>5</sup> One of the metals that is typically found associated with Nb and Ta is tin. The most important tin mineral is cassiterite (SnO<sub>2</sub>), that usually contains significant amounts of both Nb and Ta compounds. During the extraction and refining stages of the tin production, the major part of such elements remains in the final slag of the industrial process. Such slags can already be considered as an eventual and important source of refractory metals as tantalum and niobium.<sup>4</sup> Indeed, tantalum production from tin slag in Thailand and Malaysia represented 13% of the total tantalum production in 2010.<sup>6</sup> Therefore, the circularity of this kind of metals is specially important.<sup>7</sup>

In Europe, more specifically in Spain, Penouta Mine (Galicia, Spain), exploited by Strategic Minerals Spain S.L., generates Sn–Nb–Ta concentrates. However, the small grain size of the Ta–Nb minerals at the Penouta mine, and their strong association with cassiterite, make it hard to obtain separate concentrates; new methods that can separate the Sn and Nb–Ta are therefore required.<sup>8</sup> The most used technique for the separation of both metals is solvent extraction employing different agents.<sup>9,10</sup> For example, Ta could be recovered by using a simple primary amide reagent.<sup>11</sup>

Niobium and tantalum are two transition metals almost always paired together in nature, with similar physical and chemical properties. Niobium has a high melting point, relatively low density, and important magnetic and superconducting properties. Tantalum has a high thermal and

<sup>a</sup>National Center for Metallurgical Research (CENIM), Spanish National Research Council (CSIC), Avda. Gregorio Del Amo, 8, 28040 Madrid, Spain. E-mail: f.lopez@csic.es

<sup>b</sup>Department of Materials Physics, Faculty of Physics, Complutense University of Madrid, 28040, Madrid, Spain

† Electronic supplementary information (ESI) available. See DOI: 10.1039/d0ra03331f



electrical conductivity and it is well known for its high resistance to acidic corrosion. These special properties determine their primary uses.<sup>1</sup>

In a previous work,<sup>8</sup> a concentrate obtained from mining tailings containing mainly cassiterite and columbo tantalite was reduced for the production of tin metal. The recovery of Sn was >95% with a purity of 96%. A slag equivalent to 25% of the mass of the initial concentrate was produced during the recovery of the Sn. This slag could be used as a secondary raw material for obtaining Nb and Ta. In this paper a method for obtaining oxides of niobium and tantalum from the slag is described.

## Materials and methods

### Instrumental techniques

The chemical composition of slag, precursors and final compounds was analysed by X-ray fluorescence spectroscopy (XRF) using a Bruker S8 AA spectrometer (Varian, Palo Alto, CA, USA), and by Inductively Coupled Plasma-Optical Emission Spectrometry (ICP-OES) using an Agilent ICP-OES, model 5100 VDV (Vertical Dual View). The phase compositions were characterized by X-ray diffraction analysis (XRD) using a Philips X'Pert PRO diffractometer employing Cu-K $\alpha$  radiation, with a step in  $2\theta$  of  $0.05^\circ$ . Morphological examination was carried out in a scanning electron microscope (SEM) Hitachi TM3000 (Hitachi, Tokyo, Japan) and in a field emission scanning electron microscope (FE-SEM) JEOL JSM 6500 (Jeol, Tokyo, Japan). The second one is equipped with an Oxford EDX energy-dispersive X-ray (EDX) analyser for semi-quantifying the elemental composition (FE-SEM-EDX). Also, Transmission Electron Microscopy (TEM) has been performed using a JEM 2100 HT device. Analysis of the elements (with associated errors of  $\pm 3\%$ ) in the different aqueous phases was carried out by Inductively Coupled Plasma-Optical Emission Spectrometry (ICP-OES) using an Agilent ICP-OES (Agilent Technologies, Santa Clara, CA, USA), model 5100 VDV (Vertical Dual View), whereas the corresponding concentrations in the organic phases were estimated by mass balance.

### Reagents

Cyanex 923® is a mixture of 4 tri-alkyl phosphine oxides with a composition of dioctylmonohexyl phosphine oxide (R'R<sub>2</sub>PO; 31 wt%), mono-octyl dihexyl phosphine oxide (R'2RPO; 42 wt%), tri-hexyl phosphine oxide (R'3PO; 14 wt%), and tri-*n*-octyl phosphine oxide (R3PO; 8 wt%) with low solubility in water ( $0.05 \text{ g L}^{-1}$ ) and high extraction capacity. The average molecular weight is 348 and the density ( $20^\circ\text{C}$ ) is  $800 \text{ kg m}^{-3}$ .<sup>13</sup> Cyanex 923® was used as supplied by the manufacturer (CYTEC Ind.). Solvesso 100 diluent was also used as supplied by the manufacturer (ExxonMobil Chem. Iberia) and contains >99% aromatics, boiling range  $167\text{--}178^\circ\text{C}$  and flash point  $48^\circ\text{C}$ ; all other chemicals were of AR grade.

### Methods

**Leaching.** The slag used in this work was obtained after the process of recovery of tin from tailings from Penouta mine

deposit. The slag was ground in a ball mill to reach a particle size  $X < 90 \mu\text{m}$ . The chemical and physical characterization of the slag has been presented in a previous work.<sup>8</sup> A mineral concentrate obtained by the milling, gravimetric concentration, and magnetic separation of mining tailings, containing mainly cassiterite, was used as a source material for the production of metallic tin. Strategic Minerals S.L provided the concentrate. Mineralogical analysis determined that it contained Ca-Nb-Ta oxides with different stoichiometry ( $\text{Ca}_2(\text{Nb,Ta})_2\text{O}_7$  and  $\text{Ca}(\text{Nb,Ta})\text{O}_3$ ), plus much smaller proportions of other oxides of Nb, Ta, Mn and Fe ( $(\text{Fe,Mn})_2(\text{Nb,Ta})_2\text{O}_6$ ).

Acid leaching is the most frequently used method to extract metals from slags, in both research and industrial application. This method benefits from the chemical properties of metals in aqueous solution to isolate and recover a marketable product. Using this method, valuable metals from slag are leached out by the use of inorganic acids or their mixtures, *e.g.*  $\text{H}_2\text{SO}_4$ ,  $\text{HNO}_3$ ,  $\text{HCl}$ ,  $\text{HF}$ .

For the extraction of Nb and Ta, fluoride media have been extensively studied. Actually, it was the first industrial process for the extraction and purification of Nb and Ta, called Mari-gnac's process. This process allowed the production of high purity compounds but required concentrated  $\text{HF}$  solutions. The main advantage of these processes for the metals under focus in this work is that Nb(v) and Ta(v) are highly soluble in fluoride media.<sup>12</sup>

Niobium and tantalum can exist in several valence states such as +5, +4, +3, +2 and even +1 in their compounds. However, only Nb(v) and Ta(v) are stable states in solution.<sup>13</sup> Complex formation is vital for the successful separation of Ta and Nb from their mineral ores, and  $\text{HF}$  could be used both as solvent and as complexing agent<sup>14</sup> (eqn (1)):



Hydrofluoric acid is normally used in combination with sulphuric acid for the digestion of tantalum and niobium concentrate,<sup>15</sup> yielding the binary system that is used as leaching solution in this work.

Previous laboratory studies carried out by the authors<sup>16</sup> (see Table S1†), concluded that the best conditions for the leaching of the slag in the binary acid system were  $[\text{HF}] = 6 \text{ N}$  and  $[\text{H}_2\text{SO}_4] = 8 \text{ N}$ , reaction time of 3 hours and room temperature. Different slag/leaching solutions ratios were tested: 20, 30, 40, 50, 60, 75 and  $100 \text{ g L}^{-1}$ . The yield of leaching was calculated according to eqn (2):

$$Y(\% \text{wt}) = 100 - \frac{m_r \times C_r^{\text{Me}}}{m_0 \times C_0^{\text{Me}}} \times 100 \quad (2)$$

where  $m_0$  was the initial weight of the slag,  $m_r$  the weight of insoluble residue,  $C_0^{\text{Me}}$  the initial concentration (in %wt) of the metal (Me = Nb/Ta), and  $C_r^{\text{Me}}$  the concentration of the metal in the insoluble residue.

**Liquid-liquid extraction.** After leaching, the metals of interest need to be separated from the rest of the metals present in the leachate. Liquid-liquid extraction is the most effective way of separating tantalum and niobium, both metals are



extracted and separated from acidic leach liquors by using organic extractants such as methyl iso-butyl ketone (MIBK), tri-butyl phosphate (TBP), cyclohexanone and 2-octanol.<sup>13</sup> Alternative extractants have been also investigated, such as 1-octanol, that shows better characteristics than MIBK from the safety point of view.<sup>17</sup>

In the present investigation, liquid-liquid extraction experiments were performed using an organic phase of 35% (v/v) Cyanex 923® in Solvesso. Extractions were performed by shaking aliquots of Cyanex 923® and aqueous phases at 25 °C for 5 min. Aqueous to organic phase ( $V_{aq}/V_{org}$ ) volumetric ratio of 1 has been used. The solution was kept for 5 min to allow the separation of both phases. A scheme of the process is shown in Fig. 1.

Distribution ratio ( $D$ ) values and extraction efficiency ( $E$ ) values were calculated according to eqn (3) and (4) respectively:

$$D = \frac{[Me]_{org}}{[Me]_{aq}} \quad (3)$$

where  $[Me]_{org}$  was the metal concentration in organic phase at equilibrium and  $[Me]_{aq}$  the metal concentration in the aqueous phase, also at equilibrium.

Table 1 Leaching step yields at various  $s/l$  ratios

Slag/leaching solution ratio ( $g\ L^{-1}$ )	Yield (%wt)		$[Me]\ (g\ L^{-1})$	
	Nb <sub>2</sub> O <sub>5</sub>	Ta <sub>2</sub> O <sub>5</sub>	Nb	Ta
20	89.1	89.7	$1.6 \pm 0.2$	$1.9 \pm 0.2$
30	85.6	88.2	$2.3 \pm 0.3$	$2.8 \pm 0.2$
40	91.9	91.7	$3.2 \pm 0.2$	$3.9 \pm 0.3$
50	88.7	88.3	$3.6 \pm 0.2$	$4.3 \pm 0.2$
60	84.1	83.7	$4.1 \pm 0.7$	$5.0 \pm 0.9$
75	88.4	88.0	$6.0 \pm 0.2$	$7.0 \pm 0.6$
100	87.2	86.6	$7.41 \pm 0.64$	$9.43 \pm 0.96$

The percentage of metal extraction was calculated as:

$$E(\%) = \frac{[Me]_{org}}{[Me]_{aq0}} \times \frac{V_{org}}{V_{aq}} \times 100 \quad (4)$$

where  $[Me]_{org}$  was the metal concentration in organic phase,  $[Me]_{aq0}$  the metal concentration in the initial aqueous phase or leachate, before extraction,  $V_{aq}$  was the volume of aqueous phase,  $V_{org}$  was the volume of organic phase.

The separation factor ( $\beta$ ) was calculated according to:

$$\beta = \frac{D_{Me1}}{D_{Me2}} \quad (5)$$

where  $D_{Me1}$  was the distribution ratio of metal 1, e.g. Nb, and  $D_{Me2}$  the distribution ratio of metal 2, e.g. Ta.  $\beta > 1$  indicates that two metals can be separated, however gives no indication about the easiness or difficulty of the process.

**Stripping.** The stripping solution used for the selective separation of niobium was of  $NH_4F\ 0.3\ mol\ L^{-1}$  and  $NH_3\ 0.1\ mol\ L^{-1}$ . Stripping experiments were performed by shaking for 5 min aliquots of tantalum and niobium organic phases (stripping solution) at 25 °C. Aqueous to organic phases ( $V_{aq}/V_{org}$ ) volumetric ratio of 1 has been used. In the case of Ta, the stripping solution had a higher alkaline composition and also a higher concentration of  $F^-$ :  $NH_4F\ 1.1\ mol\ L^{-1}$  and  $NH_3\ 0.4\ mol\ L^{-1}$ . The same operational parameters were used ( $V_{aq}/V_{org} = 1$ ,  $T = 25\ ^\circ C$  and  $t = 5\ min$ ).

Distribution ratio ( $D_{st}$ ) values and stripping efficiency ( $E_{st}$ ) were calculated according to eqn (6) and (7), separation factor ( $\beta$ ) values were calculated according to eqn (5) as mentioned above.

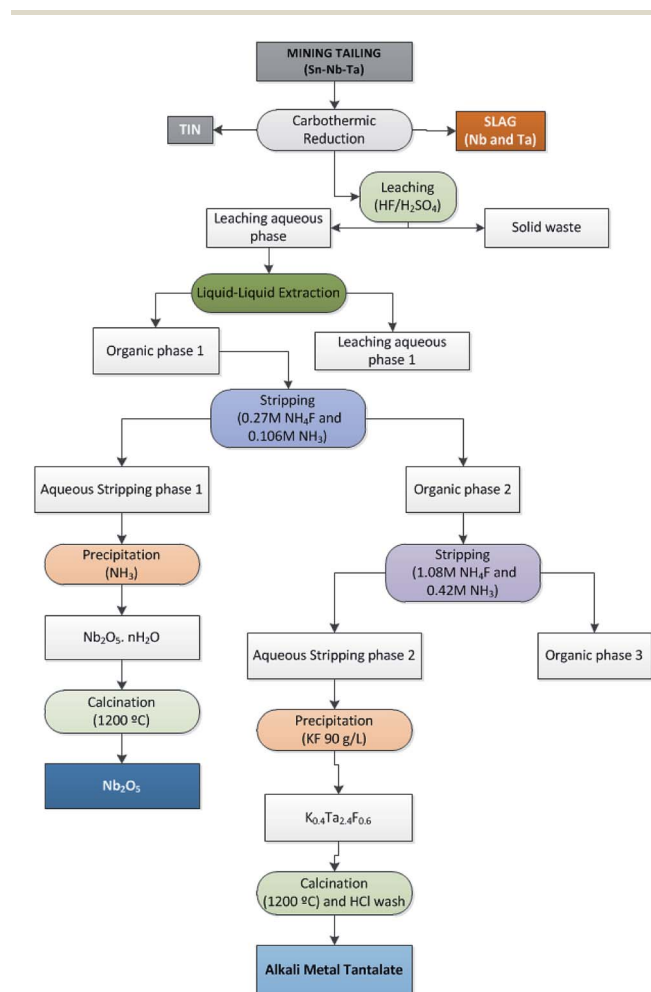


Fig. 1 Scheme of the process, including the obtaining of the slag.

Table 2 Extraction and stripping results

	Distribution ratio ( $D$ )		Extraction efficiency ( $E$ ), (%)		Separation factors ( $\beta$ )	
	Nb	Ta	Nb	Ta	Nb/Ta	Ta/Nb
Extraction	43	214	97.7	99.6	0.2	5
Stripping (Nb)	2.4	0.005	70.3	0.47	480	—
Stripping (Ta)	0.5	10.6	33.4	91.4	—	21.2



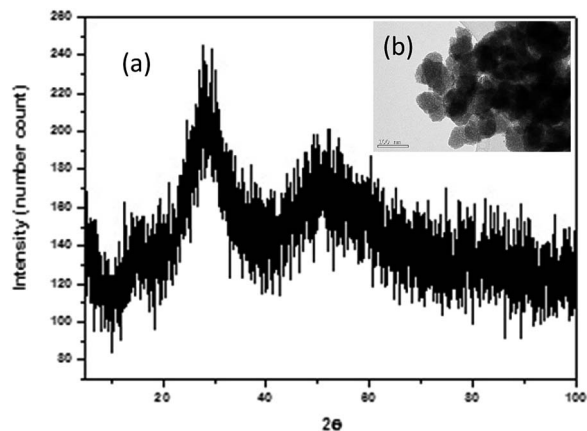


Fig. 2 (a) XRD pattern of Nb precursor. In the inset (b), a TEM of the nanoparticles is presented (scale bar of 100 nm).

$$D_{st} = \frac{[Me]_{aq}}{[Me]_{org}} \quad (6)$$

$$E_{st}(\%wt) = \frac{C_r^{Me}}{C_0^{Me}} \times \frac{V_{aq}}{V_{org}} \times 100 \quad (7)$$

In the equations above,  $[Me]_{aq}$  and  $[Me]_{org}$  were the metal concentration in the equilibrated strip phase and in organic phase at equilibrium;  $C_0^{Me}$  and  $C_r^{Me}$  were the metal concentration (Me = Nb/Ta) in the organic phase before and in the aqueous solution, and  $V_{aq}$  and  $V_{org}$  were the volumes of aqueous and organic phase respectively.

**Precursor generation.** After the separation of Nb and Ta in two different aqueous solutions, solid precursors were obtained by precipitation. For the synthesis of niobium compounds, ammonia,  $[NH_3] = 17.7 \text{ mol L}^{-1}$ , in different proportions was employed (Table S4†). For tantalum compounds, solid precursors were obtained by precipitation, using KF in different concentration as precipitating agent (Table S5†).

## Results and discussion

### Leaching of slag

The leaching of the slag was performed using a binary acid system ( $[HF] = 6 \text{ N}$  and  $[H_2SO_4] = 8 \text{ N}$ ) during 3 hours and at room temperature to ensure the greater amount of Nb and Ta leached. Insoluble residues, about 30–40% weight (Table S3†), for each ratio were analysed by XRF (Table S2†). The yields of the leaching for Nb and Ta, and the corresponding metal concentrations in the leachates, were shown in Table 1. An increase in the slag/leaching solution ratio did not modify the leaching yield. The results indicate that the HF and  $H_2SO_4$



Fig. 3 (a) XRD pattern of anhydrous niobium oxide and the identified patterns. In the inset (b), a TEM image of the crystalline particles is shown (scale bar of 0.5  $\mu\text{m}$ ).

concentration used are adequate to reach the maximum Nb and Ta leaching. All slag/leaching solution ratios showed a high yield, between 84 and 92% for both metals, so a ratio of 100 g  $L^{-1}$  was chosen as optimal conditions regarding the optimization of the process and to minimize the water waste.

It was determined that the best leaching parameters were: leaching agent: HF 6 N and  $H_2SO_4$  8 N, pulp density: 100 g  $L^{-1}$  and reaction time: 3 h. The yields obtained in the leaching step were around 87% for both metals Nb and Ta; the insoluble residue still contained around 13% of the initial content of each metal in the slag, almost independent of slag/leaching solution ratio, which is due to several reasons, including mineralogical, morphological and chemical limitations, inherent to the process.

### Separation of Ta and Nb from leachate solution

**Extraction of Nb and Ta.** Liquid–liquid extraction was performed according to the process described above. The results of this extraction in terms of distribution ratio ( $D$ ) values (eqn (3)), as well as extraction efficiency ( $E$ ) (eqn (4)), and separation factor ( $\beta$ ) values (eqn (5)), were reported in Table 2.

According to Nete *et al.*<sup>14</sup> the conversion of the fluoride anions to the neutral acids was the controlling step for the selective separation process of Nb and Ta in the organic extractant.

Accordingly with Wilson *et al.*<sup>10</sup> in highly acidic solutions, the oxygen atom of phosphine oxides protonated, *i.e.*  $R_3POH^+$ , and the as-formed protonated species extracted the metal salts by formation of ion-pair compounds, and transferring them to the organic solution. Thus, in the present case, a tentative

Table 3 Chemical composition of anhydrous niobium oxide determined by XRF (expressed as a percentage of oxides, %wt)

Oxide	Nb <sub>2</sub> O <sub>5</sub>	Ta <sub>2</sub> O <sub>5</sub>	CaO	MnO	Fe <sub>2</sub> O <sub>3</sub>	WO <sub>3</sub>	Al <sub>2</sub> O <sub>3</sub>	ZrO <sub>2</sub>	SnO <sub>2</sub>	MgO	TiO <sub>2</sub>	SiO <sub>2</sub>	NiO	ZnO
%wt)	95.1 ± 2.9	1.8 ± 0.1	0.6 ± 0.02	0.8 ± 0.02	0.6 ± 0.02	0.3 ± 0.01	0.2 ± 0.006	0.2 ± 0.007	0.1 ± 0.004	0.09 ± 0.003	0.07 ± 0.002	0.06 ± 0.002	0.01 ± 0.003	0.01 ± 0.003





**Table 4** Chemical composition of Ta precursor determined by XRF (expressed as a percentage of oxides, %wt)

Sample	Ta <sub>2</sub> O <sub>5</sub>	K <sub>2</sub> O	Nb <sub>2</sub> O <sub>5</sub>	CaO	SnO <sub>2</sub>	SiO <sub>2</sub>	Fe <sub>2</sub> O <sub>3</sub>
Ta_7	79.7 ± 2.4	17.2 ± 0.5	1.3 ± 0.04	0.8 ± 0.02	0.7 ± 0.02	0.3 ± 0.01	0.1 ± 0.003

extraction equilibrium for the extraction of tantalum(v) and niobium(v) can be written as eqn (8) and (9):



Though the involvement of additional extractant molecules in the overall stoichiometries of the extracted species cannot be discarded.

The extraction of Nb and Ta were performed using 35% (v/v) Cyanex 923® diluted in Solvesso with high yields, 97.7% for Nb, and 99.6% for Ta.

**Nb stripping.** The stripping solution used for the selective stripping and separation of niobium had the following composition: NH<sub>4</sub>F 0.3 mol L<sup>-1</sup> and NH<sub>3</sub> 0.1 mol L<sup>-1</sup>, stripping efficiency ( $E_{\text{st}}$ ), and separation factor ( $\beta$ ) values are reported in Table 2. From the results obtained, it can be observed that Ta remains in organic phase while niobium is mainly stripped to the aqueous phase, however some percentage of Nb (30%) remains in organic phase together with Ta, although part of it has been stripped in the next step. However, it should be mentioned here that this situation could be remediated by the use of more than one stage and/or varying the volume phases ratios, though this investigation had not been done yet (in fact, a counter-current plant is, at the time of writing, under construction). The separation factor of Nb vs. Ta in this step was high, what indicates that the conditions employed are optimal for separate both metals from the organic solution.

**Ta stripping.** In the case of Ta, the stripping solution has a higher alkaline composition and also a higher concentration of F<sup>-</sup>: NH<sub>4</sub>F 1.1 mol L<sup>-1</sup> and NH<sub>3</sub> 0.4 mol L<sup>-1</sup>. The same operational parameters that in Nb stripping were used ( $V_{\text{aq}}/V_{\text{org}} = 1$ ,  $T = 25^\circ\text{C}$  and  $t = 5$  min). The results are collected in Table 2. After this stripping stage more than 90% of the initial Ta was recovered.

Thus, the Nb–Ta separation process from the leaching solution took place in three steps:

(1) Co-extraction of Nb and Ta into the organic solution as neutral fluoride complex in the case of Nb, and as fluorometalates in the case of Ta.

(2) First stripping of Nb with NH<sub>4</sub>F 0.3 mol L<sup>-1</sup> and NH<sub>3</sub> 0.1 mol L<sup>-1</sup>.

(3) Ta stripping with NH<sub>4</sub>F 1.1 mol L<sup>-1</sup> and NH<sub>3</sub> 0.4 mol L<sup>-1</sup>.

Metals stripping took place, as mentioned, in two consecutive steps. In the first step Nb was stripped from the organic phase into the aqueous solution, with a stripping efficiency of 70%. In the second step Ta was stripped into the aqueous solution, with a stripping efficiency of 91%. These three steps mechanism closely resembled to those reported in the literature.<sup>14</sup>

**Synthesis of Nb compounds.** After the separation of Nb and Ta into two different aqueous solutions, solid precursors were obtained by precipitation. For the synthesis of niobium compounds ammonia, [NH<sub>3</sub>] = 17.7 mol L<sup>-1</sup>, in different proportions was employed (Table S4†). For Nb precipitation, better yields were obtained when the molar ratio Nb/NH<sub>3</sub> were low, between 0.015 and 0.03. After precipitation, solids were filtered, washed with deionized water and dried at 80 °C for 12



**Fig. 4** (a) XRD of precursor and calcined and purified Ta compounds, (b) K<sub>6</sub>Ta<sub>10.8</sub>O<sub>30</sub> particles observed by SEM, (c) SEM image of precursor and (d) K<sub>6</sub>Ta<sub>10.8</sub>O<sub>30</sub> particles observed by SEM.



hours. The chemical and mineralogical composition of the precipitate Nb\_4 (see Table S4†), the one with better results in yield terms, was determined by XRF, XRD and SEM/EDX.

XRD of Nb precursor obtained by precipitation with  $\text{NH}_3$  was shown in Fig. 2a, it was mainly an amorphous compound, as expected for a hydrated Nb oxide ( $\text{Nb}_2\text{O}_5 \cdot n\text{H}_2\text{O}$ ).<sup>18</sup> Morphology, porous spherical nanoparticles, was determined by SEM (Fig. S1a†) and TEM (Fig. 2b). Nb precursor was calcined in a tubular furnace at 1200 °C during 4 hours in  $\text{N}_2$  atmosphere, to obtain niobium oxide. A weight loss of about 19% was found. Chemical composition determined by XRF was shown in Table 3. The niobium oxide had a purity of 98.5% and the main impurity found is Ta, 1.85% expressed as  $\text{Ta}_2\text{O}_5$ .

The most intense peaks obtained in the XRD of the niobium oxide (Fig. 2a) are associated to the pseudohexagonal phase of niobium oxide ( $\text{TT-Nb}_2\text{O}_5$ ) with ICDD no. 00-028-0317. The lattice parameters are  $a = b = 3.6070 \text{ \AA}$  and  $c = 3.9250 \text{ \AA}$ . The crystal structure of this phase is considered as a defective version of the tetragonal structure ( $\text{T-Nb}_2\text{O}_5$ ).<sup>19</sup> The tetragonal phase can be easily obtained from the TT-phase by annealing.<sup>20</sup> This  $\text{T-Nb}_2\text{O}_5$  is very interesting for the fabrication of supercapacitors.<sup>21,22</sup> Less intense peaks can be associated with  $\text{Nb}_{12}\text{O}_{29}$  (ICDD no. 04-014-6587). This is a non-stoichiometric niobium oxide with monoclinic crystal structure (space group  $A2/m$ ) and lattice parameters  $a = 15.6856 \text{ \AA}$ ;  $b = 3.8307 \text{ \AA}$  and  $c = 20.7100 \text{ \AA}$  and  $\beta = 113.0560^\circ$ . Two of the recorded peaks, located at  $20.50^\circ$  and  $25.85^\circ$ , can be related to the impurities of the precursor, in particular to crystalline  $\text{SiO}_2$  with hexagonal crystal structure (space group  $P6_222$ ) and lattice parameters  $a = b = 5.03 \text{ \AA}$  and  $c = 5.62 \text{ \AA}$  (ICDD no. 01-081-1665). It is known that one of the components of the deposit is quartz, hence the adscription of these peaks to  $\text{SiO}_2$  impurity is quite plausible. The morphology of anhydrous niobium oxide was studied by TEM (Fig. 3b and S2†), confirming the presence of the two morphologies, pseudo-hexagonal and prismatic.

**Synthesis of Ta compounds.** After the separation of Ta in the strip solution, solid precursors were obtained by precipitation, using KF in different concentration as precipitating agent. The best yield was obtained using a very low Ta/KF ratio (0.015) for  $[\text{KF}] = 90 \text{ g L}^{-1}$  (Table S5†). After precipitation solids were filtered, washed with deionized water and dried at 80 °C for 12 hours. The chemical and mineralogical composition of the precipitate Ta\_7 (see Table S5†), again with the best results in yield terms, was determined by ICP-OES, XRD and SEM/EDX. XRF results were collected in Table 4. Ta precipitation with KF results in fewer impurities compared with Nb precipitation with  $\text{NH}_3$ .

XRD measurements performed on the Ta mineralogical precursor (Fig. 4a) show that the main component was  $\text{K}_6\text{Ta}_{10.8}\text{O}_{30}$ . This compound has a tetragonal crystal structure (space group  $P4/mbm$ )<sup>23</sup> with lattice parameters, determined from a Rietveld fitting, of  $a = b = 12.58 \text{ \AA}$ ,  $c = 3.96 \text{ \AA}$ . All the peaks can be associated to the  $\text{K}_6\text{Ta}_{10.8}\text{O}_{30}$  (ICDD no. 01-70-1088), and the differences in intensity can be ascribed to the existence of some preferential orientations. No peaks related to the crystalline phases of the impurities have been detected.

Ta precursor showed rod morphology (Fig. S3a†) and agglomerates with flower-type morphology (Fig. 4b). Ta precursor was calcined at 1200 °C during 4 hours, in  $\text{N}_2$  atmosphere, to obtain alkali metal tantalate. A weight loss of about 20% was found. Chemical characterization was performed by XRF. The chemical composition of tantalum salt, expressed in percentages of oxides is  $\text{Ta}_2\text{O}_5$  82.0%,  $\text{K}_2\text{O}$  15.2% and  $\text{Nb}_2\text{O}_5$ , 1.7%. It also contained some impurities as  $\text{CaO}$ ,  $\text{SnO}_2$ ,  $\text{Fe}_2\text{O}_3$ ,  $\text{NiO}$  and  $\text{ZnO}$  below 1% (Table S6†).

In view of the high impurity content, the compound obtained was treated with  $\text{HCl}$  1.5 M at 300 °C during 1 hour, to remove the impurities. After dissolution, the solid was filtered and washed with MilliQ water, and dried at 80 °C during 12 hours. The chemical characterization after purification was shown in Table S6,†  $\text{Nb}_2\text{O}_5$  content was around 1.6% and only small quantities of  $\text{CaO}$  and  $\text{SnO}_2$  (below 0.6%) could be detected. After calcination and purification, mineralogical characterization was also performed by XRD (Fig. 4c). As in the precursor, the only mineralogical phase found was,  $\text{K}_6\text{Ta}_{10.8}\text{O}_{30}$  (ICDD no. 01-70-1088). These results were in agreement with results obtained by other authors; regarding the fact that calcination of samples at 1100 °C for 2 h to 8 h does not change the mineralogical phase.<sup>24,25</sup> The morphology of tantalum salt was studied by SEM. As shown in Fig. 4d regular rod-shaped structures have been obtained. The main differences observed between the XRD in Fig. 4a and c are the intensity of some of the reflections (for example, the peak at  $29.4^\circ$ , related to (410) planes) and their width. The peaks in the Fig. 4c diffractogram are narrower, which can be an indication of reduction in internal strain in the particles, as well as an increase in particle size. As can be seen in the SEM image of Fig. 4d, rod-shaped structures have been obtained after purification, and the mean size is bigger than the rods in Fig. 4b.

## Conclusions

The process described allows the synthesis of niobium oxides and tantalum salts from a slag obtained in a pyrometallurgy process of tin production from mining tailings containing mainly cassiterite and columbo tantalite. The process consists on an acid leaching, using  $\text{HF}/\text{H}_2\text{SO}_4$  as leaching agent, with yields around 87% for both metals. Then, a solution containing  $7.2 \text{ g L}^{-1}$  and  $9.0 \text{ g L}^{-1}$  of niobium and tantalum, respectively, fed the extraction operation using Cyanex 923 as extractant; the operation has high extraction efficiencies 97.7% (Nb) and 99.6% (Ta), which resulted in raffines containing  $0.2 \text{ g L}^{-1}$  Nb and  $0.04 \text{ g L}^{-1}$  Ta, and an organic solution of  $7.1 \text{ g L}^{-1}$  Nb and  $9.0 \text{ g L}^{-1}$  Ta, which feeds the stripping operation. In the stripping operation both metals are selectively separated, with overall efficiencies of 70% (Nb) and 91% (Ta), and resulting in an organic phase that can be recycled to a new extraction step, and stripping solutions containing  $5.0 \text{ g L}^{-1}$  Nb and  $8.2 \text{ g L}^{-1}$  Ta, which feeds the corresponding precipitation–calcination operations. The final products of the process are niobium oxide and potassium tantalum salts. Niobium oxide has a purity of 98.5% and impurities of Ta, 1.85% as  $\text{Ta}_2\text{O}_5$ . Tantalum salt, after calcination and purification, has a purity of 97.3% and



impurities of Nb<sub>2</sub>O<sub>5</sub>, around 1.6%. The limiting factor of the process is the first stripping step, above all, due to the low recovery of Nb during the stripping step. This process is an alternative source of obtention of critical raw materials, that would be produced in Europe, avoiding the dependence of exportation from outside the European Union. In future research, new less aggressive and more environmentally friendly leachates will be investigated, as well as more effective stripping solution will be tested.

## Conflicts of interest

There are no conflicts to declare.

## Acknowledgements

The authors are grateful to the Spanish Ministry of Science, Innovation and Universities for support *via* the projects ESTANNIO (RTC-2017-6629-5) and MINECO/FEDER-MAT2015-65274-R, and to Complutense University of Madrid and Santander *via* the project UCM-Santander 2019 (PR87/19-22613). B. Sotillo acknowledges financial support from Comunidad de Madrid (Ayudas del Programa de Atracción de Talento (2017-T2/IND-5465)).

## Notes and references

- 1 EU, *Report on critical raw materials and the circular economy – Publications Office of the EU*, <https://publications.europa.eu/en/publication-detail/-/publication/d1be1b43-e18f-11e8-b690-01aa75ed71a1/language-en/format-PDF/source-80004733>, accessed 18 February 2019.
- 2 P. Koltun and A. Tharumarajah, *ISRN Metall.*, 2014, **2014**, 1–10.
- 3 P. Nuss and M. J. Eckelman, *PLoS One*, 2014, **9**, e101298.
- 4 E. A. Brocchi and F. J. Moura, *Miner. Eng.*, 2008, **21**, 150–156.
- 5 F. Habashi, *Handbook of extractive metallurgy*, Wiley-VCH, 1997.
- 6 M. Filella, *Earth Sci. Rev.*, 2017, **173**, 122–140.
- 7 A. P. M. Velenturf, S. A. Archer, H. I. Gomes, B. Christgen, A. J. Lag-Brotons and P. Purnell, *Sci. Total Environ.*, 2019, **689**, 963–969.
- 8 F. A. López, I. García-Díaz, O. Rodríguez Largo, F. Polonio and T. Llorens, *Minerals*, 2018, **8**, 20.
- 9 P. A. Tasker, P. G. Plieger and L. C. West, ed. J. A. McCleverty and T. Meyer, *Metal Complexes for Hydrometallurgy and Extraction*, Pergamon, Oxford, 2003, pp. 759–808.
- 10 A. M. Wilson, P. J. Bailey, P. A. Tasker, J. R. Turkington, R. A. Grant and J. B. Love, *Chem. Soc. Rev.*, 2014, **43**, 123–134.
- 11 L. M. M. Kinsman, R. A. M. Crevecoeur, A. Singh-morgan, B. T. Ngwenya, C. A. Morrison and J. B. Love, *Metals*, 2020, **10**, 346.
- 12 British Geological Survey, *Niobium Tantalum*, 2011.
- 13 Z. Zhu and C. Y. Cheng, *Hydrometallurgy*, 2011, **107**, 1–12.
- 14 M. Nete, W. Purcell and J. T. Nel, *Hydrometallurgy*, 2014, **149**, 31–40.
- 15 R. Turgis, G. Arrachart, S. Michel, S. Legeai, M. Lejeune, M. Draye and S. Pellet-Rostaing, *Sep. Purif. Technol.*, 2018, **196**, 174–182.
- 16 I. García-Díaz, T. Llorens, F. Polonio and F. A. López, in *I Iberian Meeting on Materials Science*, Scoiemat, Gijón, Spain, 2018, pp. 1–2.
- 17 V. G. Mayorov and A. I. Nikolaev, *Hydrometallurgy*, 2002, **66**, 77–83.
- 18 L. A. Rodrigues and M. L. C. P. da Silva, *J. Non-Cryst. Solids*, 2010, **356**, 125–128.
- 19 H. Schäfer, R. Gruehn and F. Schulte, *Angew. Chem., Int. Ed. Engl.*, 1966, **5**, 40–52.
- 20 C. Nico, T. Monteiro and M. P. F. Graça, *Prog. Mater. Sci.*, 2016, **80**, 1–37.
- 21 L. Kong, C. Zhang, J. Wang, W. Qiao, L. Ling and D. Long, *ACS Nano*, 2015, **9**, 11200–11208.
- 22 V. Augustyn, J. Come, M. A. Lowe, J. W. Kim, P.-L. Taberna, S. H. Tolbert, H. D. Abruña, P. Simon and B. Dunn, *Nat. Mater.*, 2013, **12**, 518–522.
- 23 A. A. Awadalla and B. M. Gatehouse, *J. Solid State Chem.*, 1978, **23**, 349–355.
- 24 C. Lan, J. Gong, Z. Wang and S. Yang, *Mater. Sci. Eng., B*, 2011, **176**, 679–683.
- 25 J. Wang, C. Xiao, X. Wu and G. Zhang, *Chin. J. Chem.*, 2017, **35**, 189–195.

